THE JOURNAL OF BIOLOGICAL CHEMISTRY
Vol. 279, No. 45, Issue of November 5, pp. 47184–47191, 2004
Printed in U.S.A.

The Long and Short Flavodoxins

II. THE ROLE OF THE DIFFERENTIATING LOOP IN APOFLAVODOXIN STABILITY AND FOLDING MECHANISM*[S]

Received for publication, May 25, 2004, and in revised form, July 21, 2004
Published, JBC Papers in Press, August 17, 2004, DOI 10.1074/jbc.M405791200

Jon López-Llano‡§¶, Susana Maldonado§¶, Shandya Jain‖, Anabel Lostao§‡‡, Raquel Godoy-Ruiz§§, José M. Sanchez-Ruiz§§, Manuel Cortijo‖, Juan Fernández-Recio‡¶¶, and Javier Sancho‡§‖‖**

From the ‡Biocomputation and Complex Systems Physics Institute, Zaragoza University, Zaragoza, Spain, §Departamento Bioquímica y Biología Molecular y Celular, Facultad de Ciencias, Universidad de Zaragoza 50009, Zaragoza, Spain, ‖Instituto de Estudios Biofuncionales, Universidad Complutense de Madrid, Madrid, Spain, and §§Facultad de Ciencias, Departamento de Química Fisica, Universidad de Granada, 18071 Granada, Spain

Flavodoxins are classified in two groups according to the presence or absence of a ~20-residue loop of unknown function. In the accompanying paper (36), we have shown that the differentiating loop from the long-chain *Anabaena* PCC 7119 flavodoxin is a peripheral structural element that can be removed without preventing the proper folding of the apoprotein. Here we investigate the role played by the loop in the stability and folding mechanism of flavodoxin by comparing the equilibrium and kinetic behavior of the full-length protein with that of loop-lacking, shortened variants. We show that, when the loop is removed, the three-state equilibrium thermal unfolding of apoflavodoxin becomes two-state. Thus, the loop is responsible for the complexity shown by long-chain apoflavodoxins toward thermal denaturation. As for the folding reaction, both shortened and wild type apoflavodoxins display three-state behavior but their folding mechanisms clearly differ. Whereas the full-length protein populates an essentially off-pathway transient intermediate, the additional state observed in the folding of the shortened variant analyzed seems to be simply an alternative native conformation. This finding suggests that the long loop may also be responsible for the accumulation of the kinetic intermediate observed in the full-length protein. Most revealing, however, is that the influence of the loop on the overall conformational stability of apoflavodoxin is quite low and the natively folded shortened variant Δ(120–139) is almost as stable as the wild type protein. The fact that the loop, which is not required for a proper folding of the polypeptide, does not even play a significant role in increasing the conformational stability of the protein supports our proposal (36) that the differentiating loop of long-chain flavodoxins may be related to a recognition function, rather than serving a structural purpose.

The flavodoxins are well known electron transfer proteins involved in both photosynthetic and non-photosynthetic reactions that carry a non-covalently bound FMN molecule as a redox center (1, 2). Given their key biological function and a series of practical facts (*i.e.* they were among the first proteins for which x-ray structures became available (3, 4), their purification in the pre-recombinant era was relatively easy, and they are reasonably stable to handle), flavodoxins were soon found to be convenient models to investigate electron transfer and molecular recognition (1, 2) and, more recently, protein stability (5–20) and folding (18–21). Based on molecular weight and sequence comparisons, they were divided in two families: short-chain and long-chain flavodoxins (the latter containing an extra ~20-residue segment, subsequently shown in Refs. 22 and 23 to form a loop in the folded protein, as highlighted in Fig. 1 of our accompanying article (36)). Despite the wealth of structural and functional information available for several flavodoxins of either family, it is still unclear whether the differentiating loop plays a structural or a functional role in the long-chain flavodoxins. In our accompanying work (36), we study two shortened loop-lacking apoflavodoxin variants of the *Anabaena* long-chain flavodoxin and show that the loop is not required for a proper folding of the polypeptide chain. In this work, we focus on the contribution of the differentiating loop to protein stability and to the folding mechanism.

The conformational stability and/or folding kinetics of three short apoflavodoxins (two different strains of *Desulfovibrio desulfuricans* (13, 20) and *Desulfovibrio vulgaris* (18)) and two long ones (*Azotobacter vinelandii* (14–17) and *Anabaena* PCC 7119 (5–12, 21)) have been reported. The available data, which have not always been gathered under the same conditions for the different proteins, suggest (but do not prove) that the long flavodoxins could display a more complex equilibrium and folding behavior than the short ones. Here we compare the chemical and thermal stability of a well folded shortened apoflavodoxin (Δ(120–139) lacking the long loop) with that of the full-length *Anabaena* wild type one and show that the loop is essential for the formation of the previously characterized equilibrium intermediate of the thermal unfolding (8). In addition, we find that the loop is also related to the occurrence of the kinetic intermediate observed in the folding of the wild type

* This work has been supported in part by Grants BMC 2001-252, PB91-0368, BI095-2068, BIO2002-00720 and BQU/2000-1500, and BIO2000-1437 of MCYT from the Spanish Ministry of Science and Technology and FEDER funds, and by Grant P120/2001 from the Aragonese Government (Diputación General de Aragón). The costs of publication of this article were defrayed in part by the payment of page charges. This article must therefore be hereby marked "*advertisement*" in accordance with 18 U.S.C. Section 1734 solely to indicate this fact.

[S] The on-line version of this article (available at http://www.jbc.org) contains Supplemental Equations 1–6 and figure.

¶ Supported by Bask Government fellowships.

** Supported by the Spanish Ministry of Science and Technology.

‡‡ Supported by a fellowship from the Aragonese Government (DGA).

¶¶ Present address: Dept. of Biochemistry, University of Cambridge, Cambridge CB21GA, United Kingdom.

‖‖ To whom correspondence should be addressed: Dept. Bioquímica y Biología Molecular y Celular, Facultad de Ciencias, Universidad de Zaragoza, 50009 Zaragoza, Spain. E-mail: jsancho@unizar.es.

protein (21). Thus, the loop adds complexity to both the equilibrium and the folding behavior of the *Anabaena* long-chain flavodoxin. Despite these effects, we notice that the shortened protein is almost as stable as the full-length one, which means that the loop plays no significant role in the stabilization of the long-chain apoflavodoxin. The fact that the loop is neither required for a proper folding of the protein (36) nor for significantly increasing its conformational stability indicates that it does not perform any structural role and suggests that instead it could be involved in a currently unknown function, which we propose might be related to the recognition of flavodoxin partner proteins.

MATERIALS AND METHODS

Site-directed Mutagenesis: Protein Expression; Purification; and Quantitation—The methods used to prepare and quantify the shortened apoflavodoxins studied in this work are described by us (36) in the accompanying paper. The Δ(119–139)-shortened variant is close to being natively folded but is somewhat expanded. The Δ(120–139) variant is natively folded. In the two variants, the 5a and 5b β-strands have been spliced and the characteristic long loop of long-chain flavodoxins has thus been removed. The stability of the shortened variants (that lack the Trp^{120} residue, important for the fluorescence and CD spectroscopic properties of wild type apoflavodoxin) is compared with that of the W120F *Anabaena* flavodoxin single mutant throughout this work. The W120F mutant is termed pseudo wild type (pWT).[1]

Urea Denaturation—Denaturing samples of different urea concentrations were prepared in 5 mM sodium phosphate, pH 7.0. Unfolding curves were obtained from the fluorescence emission of the samples at 320 nm (excitation at 280 nm) and from circular dichroism at 222 nm. The data were analyzed assuming a two-state equilibrium and a linear relationship between free energy and urea concentration (24) using Equation 1,

$$S = \frac{(S_F + m_F D) + (S_U + m_U D)e^{-(\Delta G_w - mD)/RT}}{1 + e^{-(\Delta G_w - mD)/RT}} \quad \text{(Eq. 1)}$$

where S is the observed signal, S_F and S_U are the signals of the folded and unfolded states (m_F and m_U are slopes that describe their dependences with denaturant concentration), ΔG_w is the Gibbs energy difference between the folded and unfolded states in the absence of denaturant, D is the concentration of denaturant (urea), and m the slope of the linear dependence of ΔG on D.

Thermal Denaturation—Thermal unfolding was followed by fluorescence emission (320/360 nm ratio; excitation at 280 nm) and by CD at 222 and 291 nm. The temperature was increased from 277.2 to 358.2 K at ~1 K/min in a sealed cuvette and was measured with a thermocouple immersed in the cuvette. The buffer was 5 mM sodium phosphate, pH 7, or, when indicated, 50 mM MOPS, pH 7.0. The unfolding curves were analyzed using Equation 2 (25, 26),

$$S = \frac{(S_F + m_F T) + (S_U + m_U T)e^{-(\Delta H(1 - T/T_m) - \Delta C_p((T_m - T) + T\ln(T/T_m)))/RT}}{1 + e^{-(\Delta H(1 - T/T_m) - \Delta C_p((T_m - T) + T\ln(T/T_m)))/RT}} \quad \text{(Eq. 2)}$$

where S is the spectroscopic signal, S_F and S_U the signals of the folded and unfolded states (m_F and m_U are slopes that describe their dependences with temperature), T_m is the transition temperature, and ΔH and ΔC_p are the enthalpy and specific heat of denaturation at T_m, respectively.

Differential Scanning Calorimetry (DSC) Measurements—DSC was performed using a DASM-4 microcalorimeter with digital control (cell volume 0.47 ml) at heating rates from 0.5 to 2 K/min and protein concentration in the range of 1.0–4.0 mg/ml. An extra pressure of 1.5 atm was maintained to prevent degassing of the solutions on heating. Each sample was extensively dialyzed against the buffer before measurement. The instrumental base line was routinely recorded before or after each experiment with both cells filled with buffer and was subtracted from the scan obtained with the sample. Reversibility of the unfolding was checked by sample reheating after cooling inside the calorimetric cell and by the independence of the thermograms on the scan rate. The analysis of DSC data was performed as described previously (27) using Equation 3,

$$C_p = C_p^{in} + C_p^{ex} = \frac{\Delta H^2 K_{eq}}{RT^2(1 + K_{eq})^2} + C_{p,0} + \frac{K_{eq}}{1 + K_{eq}}\Delta C_p \quad \text{(Eq. 3)}$$

where C_p^{in} is the chemical or "internal" heat capacity of the protein in solution, C_p^{ex} is the excess heat capacity of the unfolding reaction, $C_{p,0}$ is the heat capacity of the protein in the native state, and ΔC_p is the overall heat capacity change during the denaturation reaction. The values of $\Delta G°(T)$, $\Delta H(T)$, and $\Delta S(T)$ for the reversible two-state transition were calculated using Equations 4–6,

$$\Delta H(T) = \Delta H(T_m) + \Delta C_p(T - T_m) \quad \text{(Eq. 4)}$$

$$\Delta S(T) = \Delta H(T_m)/T_m + \Delta C_P \ln(T - T_m) \quad \text{(Eq. 5)}$$

$$\Delta G°(T) = \Delta H(T) - T\Delta S(T) \quad \text{(Eq. 6)}$$

where T_m is the mid-denaturation temperature, and ΔC_p was assumed to be independent of temperature. Some of the experiments were additionally performed using a VP-DSC calorimeter from Microcal (Northhampton, MA) and were analyzed assuming a linear dependence of the heat capacities of the native and unfolded states.

Stopped-flow Kinetics of Unfolding and Refolding—Stopped-flow kinetics of Δ(120–139) urea unfolding and refolding were carried out in an Applied Photophysics stopped-flow instrument. In the unfolding experiments, one volume of the protein (22 μM in 5 mM sodium phosphate buffer, pH 7.0) was mixed with 10 volumes of denaturant (urea at different concentrations in 5 mM sodium phosphate, pH 7.0). In the refolding experiments, one volume of the protein (22 μM in 5 mM sodium phosphate, pH 7, containing urea 4 M) was mixed with 10 volumes of urea at different concentrations in the same buffer. The time dependence of the change in fluorescence emission at wavelength >335 nm was recorded after excitation at 280 nm. Experimental relaxation rates and amplitudes were globally fitted as described for wild-type apoflavodoxin (21) to the equations derived for all of the possible kinetic models of a three-state system.

Statistical Analysis—To determine the statistical significance of the differences observed among the proteins studied, the equilibrium unfolding data were analyzed by paired Student's *t* tests, ANOVA, MANOVA, and correlation procedures using SPSS for Windows, release 10.0.6.

RESULTS

Equilibrium Urea Denaturation of Δ(119–139)- and Δ(120–139)-shortened Apoflavodoxins—The conformational stability of Δ(119–139) and Δ(120–139) has been determined by urea denaturation monitored by fluorescence and far-UV CD. Both shortened flavodoxins refold after unfolding in a fully reversible manner (data not shown). In addition, the unfolding equilibrium is protein concentration-independent in the 1–10 μM range and shows the same urea dependence when monitored by fluorescence or by far-UV CD (see Fig. 1), which strongly suggests that it is a two-state process. The unfolding curves have thus been fitted to Equation 1, and the parameters obtained (ΔG_w, m and $U_{½}$) are reported in Table I. The two shortened apoflavodoxins have significantly different ΔG_w values, and they are only slightly (although statistically significantly) less stable than the pWT protein (by ~3.0 and 5.5 kJ mol^{-1}). The m-slope values of the shortened apoflavodoxins are significantly smaller than those of pWT, as it is expected for smaller proteins since the m-values are related with the amount of protein surface exposed to solvent upon unfolding. The slightly expanded Δ(119–139) variant unfolds at a lower urea concentration, and therefore, it is less stable than the natively folded Δ(120–139) (see López-Llano *et al.* (36) for structural details of the two variants).

Thermal Denaturation of Δ(119–139)- and Δ(120–139)-shortened Apoflavodoxins—The thermal denaturation of the two shortened flavodoxins is also reversible (data not shown) and has been studied by fluorescence and circular dichroism in the far-UV (Figs. 2*A* and 3). In addition, the thermal unfolding of Δ(120–139) has also been studied by near-UV absorbance and

[1] The abbreviations used are: pWT, pseudo wild type; MOPS, 4-morpholinepropanesulfonic acid; DSC, differential scanning calorimetry; ANOVA, analysis of variance.

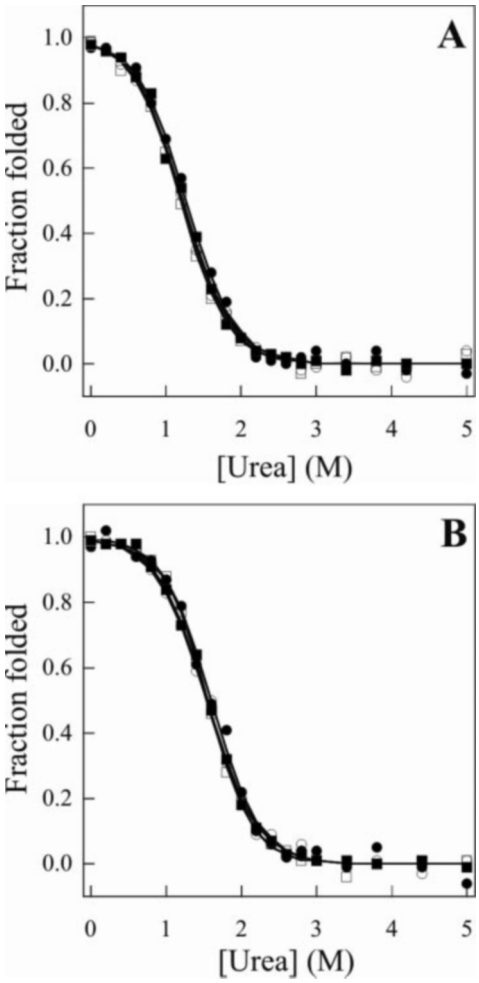

FIG. 1. **Urea denaturation of shortened apoflavodoxins in 5 mM sodium phosphate, pH 7.0.** *A*, Δ(119–139). *B*, Δ(120–139). *Open circles*, far-UV circular dichroism at 1 μM protein concentration; *open squares*, far-UV circular dichroism at 10 μM protein concentration; *solid circles*, fluorescence at 1 μM protein concentration; *solid squares*, fluorescence at 10 μM protein concentration. The *lines* are fits to a two-state equation and represent fractions of folded protein.

near-UV CD (Fig. 2*B*). Two different buffer conditions have been used: 5 mM sodium phosphate and 50 mM MOPS. The unfolding curves have been fitted to a two-state model (Equation 2) to obtain T_m and $\Delta H(T_m)$ values that are reported in Table II. Spectroscopically determined ΔC_p values usually display large errors (24) and are not reported. The thermal denaturation of the pWT protein, previously analyzed in 50 mM MOPS buffer (8, 9), has now been analyzed in 5 mM sodium phosphate to compare its stability with that of the shortened apoflavodoxins (Table II). For each of the three proteins, there are not statistically significant differences among the T_m and ΔH values obtained with the different techniques used, which implies that each protein unfolds in a two-state manner in 5 mM phosphate buffer. In addition, there is not statistically significant differences between the temperature of mid-denaturation and the unfolding enthalpies of the natively folded Δ(120–139) and of pWT, whereas Δ(119–139) is significantly less stable (as previously observed in urea denaturation). We notice that the two-state unfolding of pWT in 5 mM phosphate buffer is in contrast with the three-state unfolding in 50 mM MOPS shown by pWT (8) and by over 30 full-length apoflavodoxin mutants previously analyzed in the laboratory (data not shown). To investigate a possible role of the long loop in the accumulation of the thermal intermediate that is observed in MOPS buffer for the wild type protein, we have determined the thermal unfolding curves of natively folded Δ(120–139) in 50 mM MOPS. In addition, we have reexamined the unfolding of the pWT in MOPS buffer. Our data indicate (Table II) that the unfolding of the shortened protein in 50 mM MOPS buffer is also two-state and confirms our previous report that, in contrast, the pWT thermal unfolding in this buffer is three-state as shown by the significantly different T_m ($p < 0.05$) values obtained from the near-UV CD curve compared with the T_m values derived from the other techniques (we notice that the near-UV CD and the absorbance curves are obtained simultaneously from a single unfolding experiment). The long differentiating flavodoxin loop, absent in Δ(120–139), is thus essential for the accumulation of the apoflavodoxin thermal intermediate.

Calorimetry of Δ(119–139)- and Δ(120–139)-shortened Apoflavodoxins—A calorimetric study of the truncated flavodoxins has been carried out to determine ΔC_p. Under equilibrium conditions indicated by the independence of the thermograms on the scan rate, single reversible (to ~85–90%) endothermic peaks were obtained for either of the two variants (Fig. 4). The van't Hoff enthalpy change of denaturation at T_m (ΔH_{vH}) has been calculated for the two shortened variants under several pH and ionic strength conditions using Equation 7,

$$\Delta H_{vH} = 4RT_m^2 C_{pm}/\Delta H_m \qquad \text{(Eq. 7)}$$

where ΔH_m is the calorimetric enthalpy and C_{pm} is the maximum excess heat capacity relative to the base line at the transition temperature. The mean value of the cooperative index, η, defined as $\Delta H_{vH}/\Delta H_m$, is found at 0.98 ± 0.2 for both variants, which suggests their thermal unfolding is two-state. Nevertheless, since wild type apoflavodoxin and many full-length mutants thereof populate an equilibrium intermediate in the thermal unfolding under certain solution conditions, we have performed alternative three-state fittings of the thermal transitions as previously described (8). The three-state fittings for the shortened apoflavodoxins are not significantly better that the two-state fittings (data not shown), which agrees with the two-state behavior observed in the spectroscopically monitored thermal unfolding. As reported for the wild type protein (5), the thermograms of the shortened variants hardly change from pH 6.0 to 8.0 (data not shown); therefore, we will only report the data obtained at pH 7.0. At this pH, the observed T_m and ΔH_m of the slightly expanded Δ(119–139) are, as expected, somewhat lower than those of Δ(120–139) (see Table III). Both the T_m and ΔH_m of the two variants increase as the concentration of KCl is raised (Table III). A 1 M KCl concentration increases the T_m by 10.7 and 12.2 K for Δ(120–139) and Δ(119–139), respectively, which is similar to the effect exerted on the wild type protein (5). Plots of the enthalpy changes *versus* T_m (using data obtained at different ionic strength values) yield straight lines with ΔC_p slopes of 4.4 and 4.3 kJ K^{-1} mol^{-1} for Δ120–139 and Δ119–139, respectively (data not shown). Additionally, we have estimated (28) from extrapolations of the pre-transition and post-transition bases lines of the thermograms (data not shown) the ΔC_p values for Δ(120–139) and Δ(119–139) at 5.9 and 5.0 kJ $K^{-1}mol^{-1}$, respectively. With this and the integrated Gibbs-Helmholtz equation (Equation 8),

$$\Delta G(T) = \Delta H_m(1 - T/T_m) + \Delta C_p[(T - T_m) - T\ln(T/T_m)] \qquad \text{(Eq. 8)}$$

the stabilities at 298.2 K of Δ(120–139) and Δ(119–139) are calculated at 12.7 and 7.8 kJ mol^{-1}, respectively, which agrees fairly well with the data derived from the urea denaturation experiments (Table I). Similar stability values of 10.8 and 7.0 kJ mol^{-1} are calculated when the ΔC_p values obtained from the thermogram base lines are used. As for the effect of the ionic

TABLE I
Urea denaturation of Δ(119–139)- and Δ(120–139)-shortened apoflavodoxins and of the pseudo wild type (W120F) full-length protein

	Fld Δ(119–139)[a]		Fld Δ(120–139)[a]		W120F[a]	
	Fluorescence	CD	Fluorescence	CD	Fluorescence	CD
ΔG_w	9.71 ± 1.38[b]	9.58 ± 1.34[b]	12.26 ± 2.09[b]	11.34 ± 1.34[b]	15.36 ± 0.42	14.90 ± 0.96
kJ mol^{-1}	9.79 ± 1.38[c]	9.50 ± 1.30[c]	11.97 ± 0.96[c]	13.10 ± 0.92[c]		
m	7.62 ± 0.71[b]	7.87 ± 0.71[b]	7.74 ± 0.50[b]	7.37 ± 0.67[b]	9.42 ± 0.21	9.67 ± 0.54
kJ mol^{-1} M^{-1}	7.95 ± 0.75[c]	7.95 ± 0.67[c]	7.66 ± 1.05[c]	8.45 ± 0.50[c]		
$U_{½}$	1.27 ± 0.13[b]	1.22 ± 0.12[b]	1.60 ± 0.15[b]	1.54 ± 0.13[b]	1.63 ± 0.01	1.54 ± 0.02
M	1.23 ± 0.14[c]	1.20 ± 0.12[c]	1.54 ± 0.12[c]	1.55 ± 0.12[c]		

[a] At 298.2 ± 0.1 K in 5 mM sodium phosphate, pH 7. The means ± S.E. are provided by the fitting program.
[b] 1 μM protein concentration.
[c] 10 μM protein concentration.

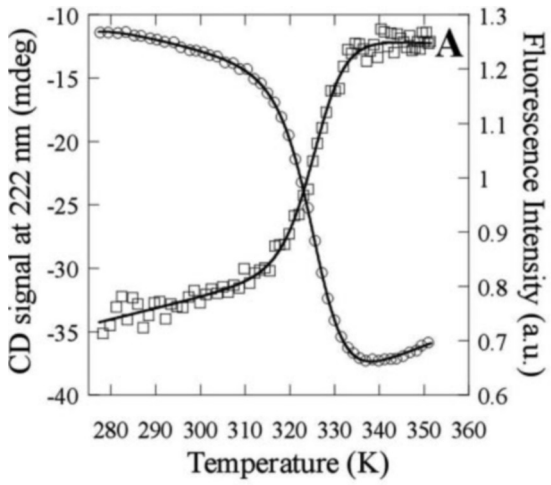

FIG. 2. **Thermal denaturation of Δ(120–139) apoflavodoxin in 5 mM sodium phosphate, pH 7.0 followed by fluorescence (ratio of intensities 320/360 nm; excitation at 280 nm: *open circles*) and far-UV CD at 222 nm (*open squares*) (*A*) and by near-UV CD (*open circles*) and near-UV absorbance at 291 nm (*open squares*) (*B*).** For practical reasons related to the instrumentation used, the absorbance values should be considered to be arbitrary units rather than actual absorbances. The *solid lines* are fits to a two-state equation. Protein concentration was 10 μM. *a.u.*, arbitrary units.

strength, we calculated (Equation 8) that, upon going from KCl 0 to 1 M, the stabilities of Δ(120–139) and Δ(119–139) increase by 6.7 and 5.9 kJ mol^{-1}, respectively. These increases are not far from the previously reported stabilizations obtained from the analysis of urea unfolding curves in different ionic strength conditions (8.4 and 6.7 kJ mol^{-1}, respectively (12)). The stabilization induced by KCl is similar to that observed for the full-length protein (12), in agreement with the fact that the removal of the loop does not alter the net charge of the protein.

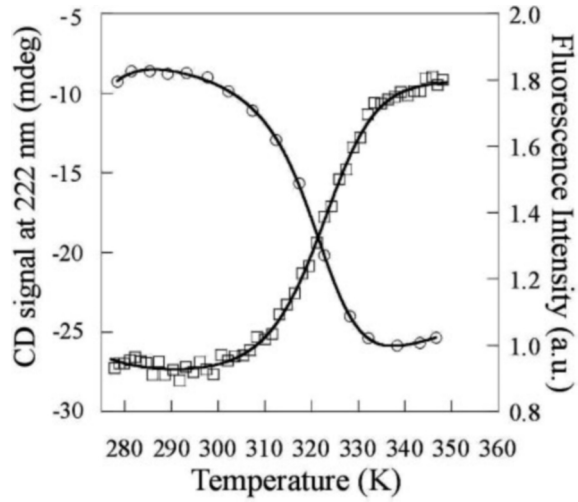

FIG. 3. **Thermal denaturation of Δ(119–139) apoflavodoxin in 5 mM sodium phosphate, pH 7.0, followed by fluorescence (ratio of emission intensities 320/360 nm; excitation at 280 nm; *open circles*) and far-UV CD at 222 nm (*open squares*).** The *solid lines* are fits to a two-state equation. Protein concentration was 10 μM. *a.u.*, arbitrary units.

Kinetics of Unfolding and Refolding of Δ(120–139)-shortened Apoflavodoxin—As reported of the wild-type protein (21), the unfolding and refolding kinetics of Δ(120–139) are biphasic, *i.e.* the data can be fitted to double exponential rate equations (data not shown). The chevron plots of the observed rate constants associated to both the fast and slow kinetic phases are quite symmetrical with the minima located around the urea concentration of mid-denaturation (Fig. 5), and the relative amplitudes of the two phases vary with urea concentration in both unfolding and refolding. Since, according to the amplitude values obtained, the entire refolding of the protein was observed, discriminating between different three-state models is possible. Thus, the whole data set of observed rate constants and amplitudes at the different urea concentrations has been globally fitted to the equations of several kinetic models. We have considered all of the possible three-state mechanisms (both linear and triangular; see Fig. 1 in Ref. 21), and the unequivocally best global fitting (R^2 = 0.935) is obtained with a triangular model displaying two interconverting native states that are populated at low denaturant concentrations (Fig. 5*A*). For this mechanism, the equations of the relaxation rates (λ_1 and λ_2) and reduced amplitudes (normalized between 0 and 1 as described previously (21)) are shown as supplemental data. The values of the fitted microscopic rate constants at 0 M urea (k_i^0) are shown in Fig. 5*A*. The relative fluorescence is F_{N_2} = 0.97 ± 0.08 (with F_{N_1} = 1 and F_D = 0).

DISCUSSION

Conformational Stability of the Shortened Apoflavodoxins: the Role of the Long Differentiating Loop in the Overall Apofla-

TABLE II
Thermal denaturation of Δ(119–139)- and Δ(120–139)-shortened apoflavodoxins and of the pseudo wild type (W120F) full-length protein

Protein[a]	Monitoring	5 mM Sodium phosphate, pH 7		50 mM MOPS, pH 7	
		T_m	ΔH	T_m	ΔH
		K	*kJ mol*$^{-1}$	*K*	*kJ mol*$^{-1}$
Δ(119–139)	Fluorescence	320.0 ± 1.2	137 ± 22		
		320.4 ± 1.3[b]	140 ± 24[b]		
	CD (far-UV)	321.4 ± 0.3	142 ± 5		
Δ(120–139)	Fluorescence	325.1 ± 0.1	232 ± 2	330.4 ± 0.1	230 ± 3
		326.0 ± 0.7[b]	224 ± 13[b]		
	CD (near-UV)	325.7 ± 0.4	245 ± 13	330.8 ± 0.6	164 ± 8
	CD (far-UV)	325.5 ± 0.1	244 ± 2	330.9 ± 0.1	244 ± 3
	Absorbance	325.1 ± 0.1	220 ± 2	331.1 ± 0.1	217 ± 1
W120F	Fluorescence	325.4 ± 0.1	224 ± 1	328.3 ± 1.0[c]	202 ± 4[c]
	CD (near-UV)	324.3 ± 0.4	222 ± 17	325.7 ± 0.5[c]	167 ± 11[c]
	CD (far-UV)	325.4 ± 0.1	229 ± 3	329.6 ± 0.5[c]	208 ± 11[c]
	Absorbance	325.4 ± 0.1	214 ± 1	329.5 ± 0.1[c]	227 ± 28[c]

[a] Means ± S.E. provided by the fitting program (Origin 7.0, Originlab Corp). 1 μM protein concentration.
[b] 10 μM protein concentration.
[c] Mean ± S.E. of two determinations.

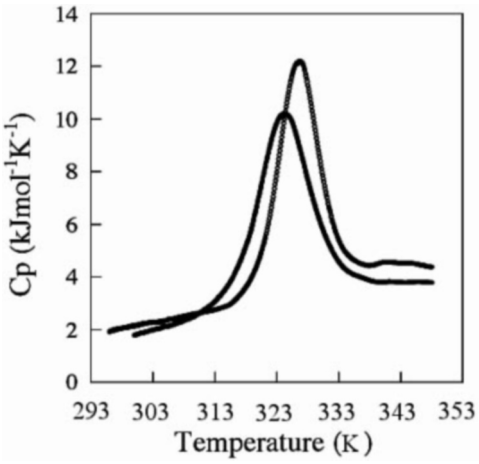

FIG. 4. **Thermal denaturation of shortened apoflavodoxins (60 μM) in 5 mM sodium phosphate, pH 7.0, by differential scanning calorimetry.** *Solid circles*, Δ(119–139); *open circles*, Δ(120–139).

vodoxin Stability and in the Stability of the Equilibrium Intermediate—The conformational stability of the apoflavodoxins of several species has been investigated, and it seems to be generally low (5–20). As for the stability of the holoform (carrying the FMN cofactor), there have been divergent reports pointing to either a significant or a rather marginal stabilization imparted by the presence of the prosthetic group (13, 18). In this work, we use the *Anabaena* model to investigate the role played by the long loop characteristic of long-chain flavodoxins on the stability of the apoprotein. To that end, the stability of two shortened apoflavodoxins variants, Δ(119–139) and Δ(120–139), has been studied by both urea and thermal denaturation. In the accompanying paper (36), we have shown that one of these variants, Δ(120–139), displays a native structure, whereas the other one, Δ(119–139), is close to being natively folded but presents local unfolding, possibly in a α-helical region. According to our analysis, the urea denaturation of either variant is fully reversible, protein concentration-independent, and can be fitted to a two-state model as indicated by the superposition of the fluorescence and far-UV CD urea-unfolding curves (Fig. 1). Thus, both variants behave in this respect similarly to wild type apoflavodoxin and to the many single mutants thereof that have been previously analyzed in our laboratory, including the W120F mutant (pWT) that has been used as a reference throughout this work. As for the overall conformational stability, the two shortened apoflavodoxins lacking the long loop are less stable than the pWT full-length protein, although the difference (~3.0 kJ mol^{-1} for Δ(120–139) and 5.5 kJ mol^{-1} for Δ(119–139)) is quite small, especially for the natively folded Δ(120–139). This is quite revealing, because it agrees very well with the peripheral structural role of the long loop removed, which has been illustrated in the accompanying paper (36). The loop is not essential for a proper folding of the protein and does not impart a significant stabilization (a 3-kJ mol^{-1} stabilization can be so easily obtained from simple point mutations that does not justify the presence of a 20-residue loop in a protein). The locally expanded Δ(119–139) apoflavodoxin is ~2.5 kJ mol^{-1} less stable than Δ(120–139), consistent with its observed small departure from the native state. The cooperative unfolding of Δ(119–139) illustrates that protein conformations of low stability may still behave in a highly cooperative manner toward unfolding, as previously demonstrated by the analysis of an even less structured molten globule apoflavodoxin fragment (11).

The unfolding of the shortened flavodoxins has also been studied by thermal denaturation. The spectroscopically monitored thermal unfolding has been performed in two different buffer conditions. We have initially used 5 mM sodium phosphate, which was the buffer previously used to characterize a flavodoxin fragment deprived from the C-terminal helix (11). Our data in Table II indicate that, in this buffer, Δ(119–139) is less stable than both pWT and Δ(120–139) by 4–5° and that its enthalpy of unfolding is significantly smaller. Interestingly, all of the thermal unfolding curves gathered for the three proteins give within each protein the same T_ms, which indicates that the thermal unfolding of pWT and that of its shortened versions is two-state in this buffer. This is in clear contrast with the behavior of both wild type and pWT in 50 mM MOPS (8, 9) and indicates that small differences in ionic strength and/or sodium concentration can significantly modify the population of the thermal intermediate of the pWT protein. Although this fact is not too surprising given the complex dependence of apoflavodoxin stability on ionic strength and cation concentration (12), especially at low ionic strength and low cation concentration, it has prompted us to examine whether the shortened apoflavodoxins do populate a thermal unfolding intermediate at all at the higher ionic strength and sodium concentration provided by the 50 mM MOPS buffer where WT apoflavodoxin and all of the single mutants thereof so far analyzed (including pWT) do display a thermal unfolding intermediate. To that end, we followed the thermal unfolding of Δ(120–139) in 50 mM MOPS buffer by fluorescence, near- and far-UV CD, and absorbance (Table II) and all of the techniques gave essentially the same T_m, which means that the shortened apoflavodoxin no longer populates a thermal unfolding equilibrium intermedi-

TABLE III
Thermal unfolding of Δ(120–139) and Δ(119–139) apoflavodoxins at different KCl concentrations

[KCl]	Δ(120–139)[a]					Δ(119–139)[a]				
	T_m	ΔH_m	η^b	$\Delta C_p{}^c$	$\Delta G^{0\,d}$	T_m	ΔH_m	η^b	$\Delta C_p{}^c$	$\Delta G^{0\,d}$
M	*K*	*kJ/mol*		*kJ/mol K*	*kJ/mol*	*K*	*kJ/mol*		*kJ/mol K*	*kJ/mol*
0	327.0	210	1.01	4.6 (5.9)	13.9 (10.9)	324.5	154	0.99	4.2 (5.0)	8.0 (7.1)
0.05	330.2	222	0.97			329.9	175	0.98		
0.1	332.1	232	0.96			331.0	183	0.99		
0.25	335.6	244	0.98			332.7	190	1.02		
0.5	336.7	250	1.01			334.4	198	0.96		
1.0	337.7	260	0.99			336.7	205	0.96		

[a] In 5 mM sodium phosphate, pH 7. Means ± S.D. are as follows: 0.2 K in T_m; 5% in ΔH, and 10% in ΔC_p. Protein concentration was 60 μM.
[b] $\Delta H_{vH}/\Delta H_m$, where ΔH_{vH} is given by Equation 7.
[b] ΔC_p calculated as the slope of a representation of ΔH versus T_m with the data at different KCl concentrations. The values in parentheses have been alternatively calculated from the pre-transition and post-transition base lines.
[d] Calculated at 25 °C. Values in parentheses calculated with ΔC_p values form the transition base lines.

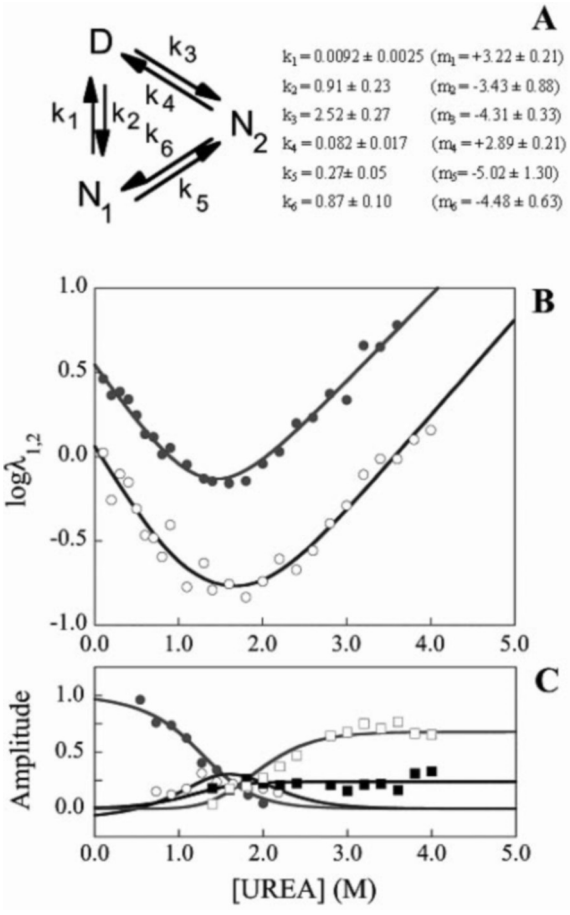

FIG. 5. Folding kinetics of Δ(120–139) apoflavodoxin globally fitted to a three-state triangular mechanism involving two interconverting native species (*scheme A*). Fitted values of the microscopic constants and their urea dependences are shown. The urea concentration dependence of the natural logarithms of the observed rate constants for unfolding (*B*, *filled circles*, fast phase; *open circles*, slow phase) and their corresponding amplitudes (*C*, *filled circles*, fast refolding phase; *open circles*, slow refolding phase; *filled squares*, fast unfolding phase; *open squares*, slow unfolding phase) are shown. The *solid lines* are the global fit of the data to the triangular mechanism (see supplemental material). The data were acquired at 298.2 ± 0.1 K in 5 mM sodium phosphate.

ate. In contrast, the pWT protein shows similar temperatures for three of the techniques but the unfolding followed by near-UV CD displays a T_m four degrees lower (well beyond the experimental error) as previously reported (8, 9). It should be noted that the near-UV CD and the absorbance curves are acquired simultaneously on the same sample and, therefore, their T_m differences are most accurately determined. Thus, our data show that the loop is essential for the occurrence of the apoflavodoxin thermal intermediate, which can be explained in two contrasting scenarios. On the one hand, it could be that, when the entire protein is heated and destabilized, remaining interactions between the loop and the rest of the protein are strong enough to prevent a global unfolding at moderate temperatures, thus contributing to stabilize an intermediate conformation. Alternatively, the loop would stabilize the native conformation relative to the intermediate so that, upon moderate heating, a local unfolding confined to the loop would trigger the conversion of the native state into the intermediate. To clarify the matter, a detailed ϕ-analysis of the structure of the thermal intermediate has been independently performed by combining information from 30 apoflavodoxin single mutants.[2] This analysis indicates that the second scenario is correct; therefore, the initial native to intermediate unfolding transition observed in the full-length apoflavodoxins represents essentially the unfolding of the long loop. This is why the shortened variants do not populate an intermediate in the thermal unfolding.

The pH and ionic strength dependences of the thermal unfolding of the shortened apoflavodoxins have been investigated by DSC. A two-state model was used to fit the thermograms, which lead to ratios of the vant'Hoff and calorimetric enthalpies close to one. Additionally, a three-state analysis of the data was tentatively performed but it did not significantly improve the fits. Both the temperatures of mid-denaturation and the enthalpy changes obtained from the DSC data are similar to those derived from the spectroscopically monitored unfolding curves and indicate that the natively folded Δ(120–139) is slightly more stable and displays a higher enthalpy of denaturation than the Δ(119–139) variant. The heat capacity changes of the two shortened variants are nevertheless similar and reflect substantial burial of hydrophobic residues in their structures. Almost no pH dependence of T_m and ΔH was noticed from pH 6 to 8. In contrast, the ionic strength effects on T_m are large. From ionic strength = 7 mM to 1 M, the temperatures of mid-denaturation increase by 11–12° in the two shortened variants, the greatest effects taking place in the low ionic strength region (see Table III). This behavior mimics the one observed in the wild type protein (12), which is greatly stabilized by salts due both to a relief of electrostatic repulsions (flavodoxin is very acidic) and to the binding of cations. From data in Table III, we estimate that the stability of the loop-lacking variants is increased in I = 1 M by around 6 kJ mol^{-1} (relative to low ionic strength), which is similar to the effect observed in the wild type protein and suggests that the cation binding sites are retained in the short variants.

[2] Campos, L. A., Bueno, M., Lopez-Llano, J., Jiménez, M. A., and Sancho, J. (2004) *J. Mol. Biol.*, in press.

The Folding Mechanism of the Shortened Δ(120–139) Apoflavodoxin: a Switch in Kinetic Mechanism Induced by the Long Loop—The folding mechanism of the well folded shortened Δ(120–139) variant has been determined by global analysis of kinetic unfolding and refolding data at different urea concentrations. The model that fits the experimental data for Δ(120–139) shares with the one found for WT apoflavodoxin the involvement of three species in a triangular arrangement (Fig. 5*A*). However, despite these similarities, the removal of the loop significantly modifies the folding mechanism and the properties of the species involved in the kinetic pathway. The transient intermediate that appears in the folding reaction of the wild type protein is essentially a kinetic trap (21). In contrast, the folding of Δ(120–139) involves three species just because two interconverting native states are populated at low urea concentration ("native" only meaning they are significantly populated at a 0 M urea). From the microscopic rate constants obtained in the global fit (Fig. 5*A*), the molar fraction of the two native states and of the unfolded state can be calculated as a function of urea concentration (see supplemental material). In the absence of denaturant, N_1 constitutes 76% of the molecules and N_2 constitutes the remaining 24%. Although the occurrence of two species in the absence of denaturant might seem to conflict with the reported two-state equilibrium urea unfolding of Δ(120–139), the fact is the two species look very similar. A two-state analysis of the urea dependence of each native species (calculated from kinetic data in Fig. 5*A*) indicates that they show similar urea concentrations of mid-denaturation and m values (for N_1: $U_{½}$ = 1.83 M and m = 7.1 kJ mol^{-1} M^{-1}; for N_2: $U_{½}$ = 1.53 M and m = 5.8 kJ mol^{-1} M^{-1}). In addition, the relative fluorescence intensities of the two species are also very similar (1 for N_1 and 0.97 for N_2). This is why a representation of the total fraction of the folded protein (N_1 plus N_2) as a function of urea concentration reproduces the observed equilibrium unfolding curve of Δ(120–139) (data not shown), which lends support to the global kinetic analysis. Indeed, the stability values calculated from the so-reconstructed equilibrium curve ($\Delta G = -12.0$ kJ mol^{-1}) and from the experimental one (Table I) are the same within error.

The degree of hydrophobic surface exposure in the different species involved (the N_1, N_2, and D states plus the three intervening transition states) can be estimated from the urea dependence of the microscopic rate constants (m_1 in Fig. 5*A*). The so-called α parameter (29) provides a qualitative estimation of the relative compactness of the different states. If we take $\alpha_U = 0$ and $\alpha_{N_1} = 1$, α_{N_2} is calculated at 1.08 ± 0.10, which means the two native states are similarly compact. As expected, the compactness of the transition states between the native species and the denatured state, $\alpha^{\ddagger}_{DN1}$ and $\alpha^{\ddagger}_{DN2}$, are markedly reduced to 0.52 ± 0.05 and 0.64 ± 0.07, respectively. More intriguing is the compactness of the transition state connecting the two native states ($\alpha^{\ddagger}_{N1N2}$ = 1.75 ± 0.22), suggestive of a greater compaction than that in the native species. Although the reason for this is not clear, an analogous phenomenon of high compactness in the transition state between two similarly compact species (N and I) was observed for the wild type protein and a possible explanation was offered (21).

The very similar fluorescence and compactness of N_1 and N_2 support a truly native character of the minor native species but do not offer clues on the differences between the states. It is clear that they are not related to the presence of associated monomers in the solution, because our exclusion chromatography experiments indicate the protein remains monomeric at least up to 200 μM, well above the concentration used in the kinetic experiments. The native species seem to be simply two slow, interconverting conformations of similar fluorescence. One possibility is that they are local alternative conformations at the region that has been spliced in order to delete the loop. If this were the case, the kinetic intermediate that complicates the folding reaction of the full-length wild type protein would have simply disappeared after loop removal. In any case, it is clear that the occurrence of the wild type apoflavodoxin-folding intermediate is strongly related to the presence of the 120–139 loop.

On the other hand, the speed of protein folding reactions seems related to the complexity of the specific native topologies. In this respect, the length of loops has been shown to correlate with observed protein folding rates (30–33) and usually longer loops give rise to slower reactions. Somewhat unexpectedly, a simple comparison of the Δ(120–139) and wild type (21) unfolding data indicates that the observed folding rate (D → N) of wild type apoflavodoxin is one order of magnitude larger than that of the most populated native state of Δ(120–139) (10.4 *versus* 0.91 s^{-1}). Although small differences in buffer composition (50 mM MOPS, pH 7.0, I = 17 for the wild type protein and 5 mM sodium phosphate, pH 7.0, I = 9 mM for Δ(120–139)) could contribute to the effect, the faster folding of the full-length protein suggests that the long loop stabilizes the transition state by lowering its enthalpy and that this effect overcomes the expected entropic destabilization associated with the presence of the long loop. Anyhow, the different folding mechanisms followed by the wild type protein and the Δ(120–139) variant exemplifies the kinetic plasticity of proteins that can switch to alternative folding mechanisms under mild or even extreme sequence alterations, as it has been previously illustrated by the folding of protein permutants (34, 35).

CONCLUSIONS

The long loop characteristic of long-chain flavodoxins influences the equilibrium folding behavior of the apoprotein. It determines the occurrence of an equilibrium intermediate in the thermal unfolding because, at moderate temperatures, the loop becomes unfolded unlike the rest of the protein. In addition, the loop is related to the accumulation of a transient intermediate in the apoflavodoxin-folding pathway. However, despite these complicating effects, the loop hardly contributes to the conformational stability of the apoprotein. The facts that the shortened apoflavodoxin can adopt a native structure and that its stability is very similar to that of the full-length protein strongly suggest that the loop is a peripheral element from both the structural and energetic points of view and support our proposal that the loop may instead play a role in flavodoxin partner recognition (36).

REFERENCES

1. Mayhew, S. G., and Tollin, G. (1992) in *Chemistry and Biochemistry of Flavoenzymes* (Müller, F., ed) Vol. III, pp. 389–426, CRC Press, Inc., Boca Raton, FL
2. Ludwig, M. L., and Luschinsky, C. L. (1992) in *Chemistry and Biochemistry of Flavoenzymes* (Müller, F., ed) Vol. III, pp. 427–466, CRC Press, Inc., Boca Raton, FL
3. Ludwig, M. L., Andersen, R. D., Mayhew, S. G., and Massey, V. (1969) *J. Biol. Chem.* **244,** 6047–6048
4. Watenpaugh, K. D., Sieker, L. C., Jensen, L. H., Legall, J., and Dubourdieu, M. (1972) *Proc. Natl. Acad. Sci. U. S. A.* **69,** 3185–3188
5. Genzor, C. G., Beldarrain, A., Gomez-Moreno, C., Lopez-Lacomba, J. L., Cortijo, M., and Sancho, J. (1996) *Protein Sci.* **5,** 1376–1388
6. Fernandez-Recio, J., Romero, A., and Sancho, J. (1999) *J. Mol. Biol.* **290,** 319–330
7. Langdon, G. M., Jimenez, M. A., Genzor, C. G., Maldonado, S., Sancho, J., and Rico, M. (2001) *Proteins* **43,** 476–488
8. Irun, M. P., Garcia-Mira, M. M., Sánchez-Ruiz, J. M., and Sancho, J. (2001) *J. Mol. Biol.* **306,** 877–888
9. Irun, M. P., Maldonado, S., and Sancho, J. (2001) *Protein Eng.* **14,** 173–181
10. Maldonado, S., Lostao, A., Irún, M.P., Fernández-Recio, J., Genzor, C. G., González, E. B., Rubio, J. A., Luquita, A., Daoudi, F., and Sancho, J. (1998) *Biochimie* (*Paris*) **80,** 813–820
11. Maldonado, S., Jimenez, M. A., Langdon, G. M., and Sancho, J. (1998) *Biochemistry* **37,** 10589–10596

12. Maldonado, S., Irun, M. P., Campos, L. A., Rubio, J. A., Luquita, A., Lostao, A., Wang, R., Garcia-Moreno, E. B., and Sancho, J. (2002) *Protein Sci.* **11,** 1260–1273
13. Apiyo, D., Guidry, J., and Wittung-Stafshede, P. (2000) *Biochim. Biophys. Acta* **1479,** 214–224
14. Steensma, E., Nijman, M. J., Bollen, Y. J., de Jager, P. A., van den Berg, W. A., van Dongen, W. M., and van Mierlo, C. P. (1998) *Protein Sci.* **7,** 306–317
15. van Mierlo, C. P., van Dongen, W. M., Vergeldt, F., van Berkel, W. J., and Steensma, E. (1998) *Protein Sci.* **7,** 2331–2344
16. Steensma, E., and van Mierlo, C. P. (1998) *J. Mol. Biol.* **282,** 653–666
17. van Mierlo, C. P., van den Oever, J. M., and Steensma, E. (2000) *Protein Sci.* **9,** 145–157
18. Nuallain, B. O., and Mayhew, S. G. (2002) *Eur J Biochem.* **269,** 212–223
19. van Mierlo, C. P., and Steensma, E. (2000) *J. Biotechnol.* **79,** 281–298
20. Apiyo, D., and Wittung-Stafshede, P. (2002) *Protein Sci.* **11,** 1129–1135
21. Fernández-Recio, J., Genzor, C. G., and Sancho, J. (2001) *Biochemistry* **40,** 15234–15245
22. Smith, W. W., Pattridge, K. A., Ludwig, M. L., Petsko, G. A., Tsernoglou, D., Tanaka, M., and Yasunobu, K. T. (1983) *J. Mol. Biol.* **165,** 737–753
23. Rao, S. T., Shaffie, F., Yu, C., Satyshur, K. A., Stockman, B. J., Marley, J. L., and Sundaralingam, M. (1992) *Protein Sci.* **1,** 1413–1427
24. Pace, C. N., Shirley, B. A., and Thomson, J. A. (1989) in *Protein Structure: A Practical Approach* (Creighton, T. E., ed) pp 311–330, Oxford University Press, Oxford
25. Privalov, P. L. (1979) *Adv. Prot. Chem.* **33,** 167–241
26. Privalov, P. L., and Potekhin, S. A. (1986) *Methods Enzymol.* **131,** 4–51
27. Beldarrain, A., Lopez-Lacomba, J. L., Furrazola, G., Barberia, D., and Cortijo, M. (1999) *Biochemistry* **38,** 7865–7873
28. Plaza del Pino, I. M., and Sanchez-Ruiz, J. M. (1995) *Biochemistry* **34,** 8621–8630
29. Roder, H., and Colon, W. (1997) *Curr. Opin. Struct. Biol.* **7,** 15–28
30. Viguera, A. R., and Serrano, L. (1997) *Nat. Struct. Biol.* **4,** 939–946
31. Ladurner, A. G., and Fersht, A. R. (1997) *J. Mol. Biol.* **273,** 330–337
32. Fersht, A. R. (1999) *Proc. Natl. Acad. Sci. U. S. A.* **97,** 1525–1529
33. Nagi, A. D., Anderson, K. S., and Regan, L. (1999) *J. Mol. Biol.* **286,** 257–265
34. Lindberg, M., Tangrot, J., and Oliveberg, M. (2002) *Nat. Struct. Biol.* **9,** 818–822
35. Li, L., and Shakhnovich, E. I. (2001) *J. Mol. Biol.* **306,** 121–132
36. López-Llano, J., Maldonado, S., Bueno, M., Lostao, A., Ángeles-Jiménez, M., Lillo, M. P., and Sancho, J. (2004) *J. Biol. Chem.* **279,** 47177–47183